POLITECNICO DI TORINO
Repository ISTITUZIONALE

Harmonic Balance TCAD Trap Modeling of GaN HEMTs for Design Technology Co-Optimization

Original
Harmonic Balance TCAD Trap Modeling of GaN HEMTs for Design Technology Co-Optimization / De Ruvo, E., Guerrieri, S.D., Bonani, F.. - ELETTRONICO. - (2026), pp. 1-3. (2026 IEEE MTT-S International Conference on Numerical Electromagnetic and Multiphysics Modeling and Optimization (NEMO) Valencia (Spa) 1-3 July 2026) [10.1109/nemo66765.2026.11622141].

Availability:
This version is available at: 11583/3014802 since: 2026-08-24T11:58:48Z

Publisher:
IEEE

Published
DOI:10.1109/nemo66765.2026.11622141

Terms of use:

This article is made available under terms and conditions as specified in the corresponding bibliographic description in the repository

Publisher copyright
IEEE postprint/Author's Accepted Manuscript

©2026 IEEE. Personal use of this material is permitted. Permission from IEEE must be obtained for all other uses, in any current or future media, including reprinting/republishing this material for advertising or promotional purposes, creating new collecting works, for resale or lists, or reuse of any copyrighted component of this work in other works.

(Article begins on next page)

10 October 2026

Harmonic Balance TCAD Trap Modeling of GaN HEMTs for Design Technology Co-Optimization

Edoardo De Ruvo, Simona Donati Guerrieri, Fabrizio Bonani
Department of Electronics and Telecommunications, Politecnico di Torino, Italy

***Abstract*—A physics-based simulation tool is presented allowing for the 2D mixed-mode, self-consistent simulation of GaN HEMTs including the full dynamic effect of traps. The model is solved in the frequency domain exploiting Harmonic Balance, and is used here to discuss the dispersive effects of traps in Class A and deep Class AB power stages developed on GaN technology, with reference to T-dependent dynamic load lines and dispersive DC current.**

***Index Terms*—AC parameter dispersion, GaN HEMTs, Nonlinear device models, TCAD simulations, Trap rate equations**

I. Introduction

Memory effects due to deep trap levels are well known to limit the deployment of GaN HEMT technology for power applications. Reliable HEMT compact models including nonlinear trap dynamics are necessary for microwave power amplifier design, but are still difficult to identify [1], [2], [3]. Technology CAD (TCAD) is an essential complement to experimental characterization to identify the trap occupation dynamics in the nonlinear device operating conditions, with the main advantage of retaining the direct link connecting the device terminal electrical characteristics to the microscopic trap distribution and physical parameters. While TCAD time-domain analysis has been extensively used [4], [5], less exploited is frequency domain TCAD. On the other hand, a frequency domain Large Signal (LS) TCAD is the ideal tool to model the device in operating conditions close to the circuit design ones, as well as to harmonic characterization benches. In this work, we present an in-house tool implementing mixed-mode, self-consistent Harmonic Balance (HB) TCAD simulations including dynamic trap rate equations. To demonstrate the software capabilities, we address for the first time the influence of the trap dynamics directly on the device dynamic load lines (DLLs) and DC dispersion of a GaN HEMT power amplifier as a function of temperature. In particular, we demonstrate that the large swing of electron density, typical of LS operation, leads to a significant variation of the trap occupation, implying a noticeable decrease of the DC drain current with increasing output power. The T-dependent parametric analysis reported in this work is a first step towards a fully self-consistent multiphysics PA self-heating TCAD analysis, akin to [6]. Furthermore, the exact knowledge of HEMT nonlinear memory effects allows for the development of a fully TCAD based power amplifier design, where the embedding circuit is substituted by physical structures from EM simulators [7].

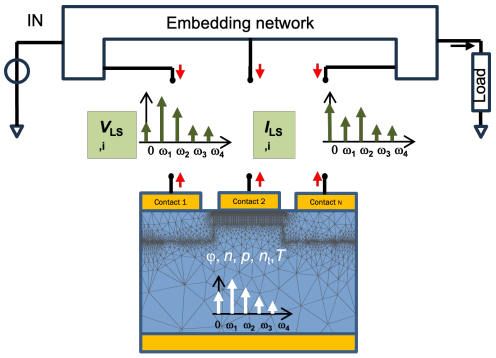

Fig. 1: Schematic representation of the software set-up for mixed-mode HB TCAD analysis. The external embedding circuit includes microwave components as ideal idlers, bias tees and harmonic tuned terminations.

Fig. 1 shows the mixed-mode setup (physical device + external circuit) of the in-house developed HB TCAD tool. Both the discretized physical device equation system and the external circuit equations are solved in the frequency domain by means of the Harmonic Balance technique. The terminal currents are balanced for each harmonic at the interconnecting ports [8], [9] (see Fig. 1). The active device is modeled by the drift-diffusion carrier transport model coupled to time-dependent trap rate equations. Traps are modeled following Shockley-Read-Hall (SRH) theory [10] as a function of trap energy, trap parameters (cross section etc.) and position in the device. Currently, traps are non interacting in terms of energy transitions, and the trap rate equations are local. In the external network, besides standard Spice components, our in-house HB-TCAD software implements ad-hoc frequency-domain defined components such as idlers, ideal bias tees and harmonic terminations. External networks can also be substituted by frequency-domain scattering matrices extracted from EM simulations, starting from a foundry simulation deck. Notice that our in-house software is unique for LS analysis because, differently from commercial HB TCAD implementations, e.g. [11], it does not make any simplifying assumption on the trap dynamics.

II. Simulations

To demonstrate the software capability, we simulate the HEMT structure shown in Fig. 2 and Table I, with dimensions chosen consistently with modern technologies [12]. Fe doping induces deep acceptor-like traps $N_{\mathrm{T}} = 10^{18}$ cm^{-3}, nominal

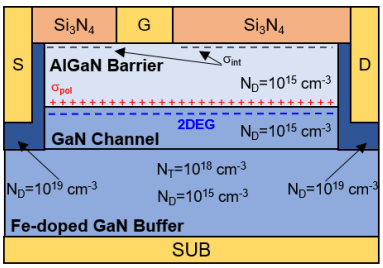

Fig. 2: Cross section of the simulated device. The gate length is 150 nm.

TABLE I: Relevant sizes for the HEMT structure under consideration

Thickness		Length	
Si_3N_4	100 nm	Gate	150 nm
AlGaN barrier	15 nm	Gate-Source	800 nm
GaN buffer	2000 nm	Gate Periphery	1 mm

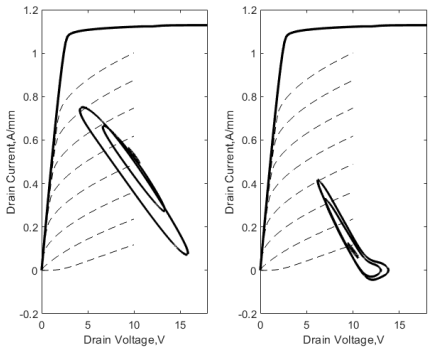

Fig. 3: DLL on the output characteristic for several input available powers: $P_{\text{av}} = -25$ dBm (almost invisible), -5 dBm, 10 dBm and 15 dBm. Left: class A bias point. Right: class AB bias point.

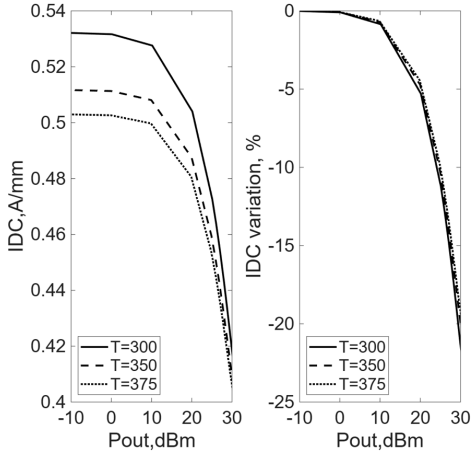

Fig. 4: Class A DC component of the LS drain current with increasing output power at the three analyzed temperatures.

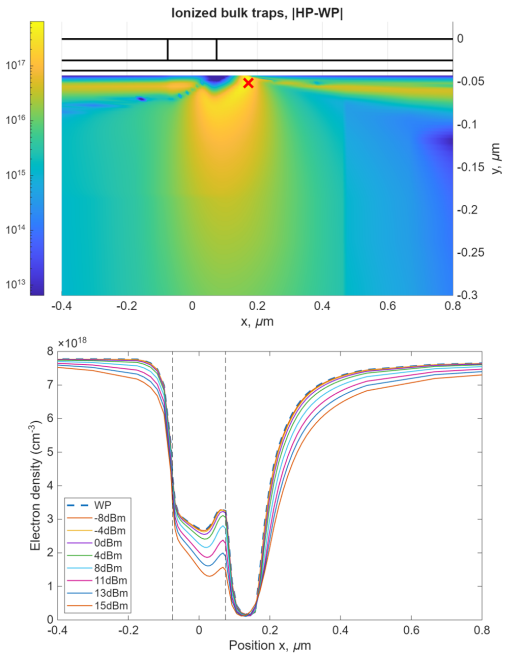

Fig. 5: Class A DC behavior. Top: difference of occupied traps DC component at available input power $P_{\text{av}} = 15$ dBm (HP) and at the DC working point (WP). The "x" represents the point investigated in Figs. 6-7. Bottom: cross section of the electron density in the channel, 1 nm below the AlGaN/GaN interface, as a function of the available power.

trap energy $0.4\,\text{eV}$ below the conduction band, and capture cross-sections $\sigma_n = \sigma_p = 3 \times 10^{-16}$ cm^2. We aim at the investigation of effects of the Fe trap occupation dynamics under LS conditions.

We address the operation of a 12 GHz power amplifier either in class A (50% of IDSS) or deep class AB (10% of IDSS) with tuned load. The selected drain bias voltage is $V_{\text{D}} = 10$ V. In both class A and AB stages, the device is terminated on the optimum tuned load $Z_{\text{L, opt}} = (16 + j3.6)\ \Omega$ at the fundamental frequency, while the input port is on $50\ \Omega$. Despite the class A case is not usual for practical power amplifier design on GaN technologies, we will demonstrate its relevance to understand LS trap-related effects.

Fig. 3 shows the output DLLs ($I_{\text{D}} - V_{\text{D}}$) with increasing power for both stages, along with the static DC curve and the simulated pulsed output characteristics (quiescent point equal to the class A working point). Both DLLs show noticeable trap-induced effects, in line with experimental reports [13]: remarkably, the class A stage shows in particular a progressive reduction of the DC current component with increasing power, an unexpected result in a class A quasi-linear stage, especially when operation is not yet in compression.

In this work, we focus on this peculiar DC behavior, which is also confirmed at high temperatures, as shown in Fig. 4. While, as expected, the DC current is very sensitive to temperature (Fig. 4 left), the relative variation from low to high power is practically insensitive to T (Fig. 4 right). To

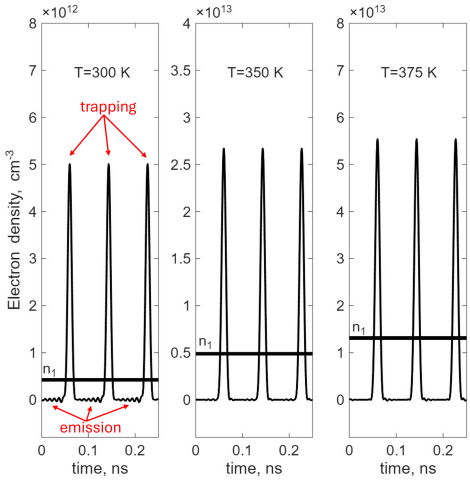

Fig. 6: Class A time domain electron density at high power ($P_{\text{out}} = 30$ dBm) in the selected point in the drain depleted region. Thick solid lines show the n_1 value (T-dependent).

understand the physical origin of this behavior, we monitor the trap occupation in the device, starting at $T = 300$ K.

As shown in Fig. 5 above, the DC component of the occupied trap density (the only harmonic component, since the trap cut-off frequency is well below 12 GHz), varies significantly from back-off to compression, in particular at the channel end, towards the drain. Also the DC component of the electron density in the channel varies significantly with increasing power, see Fig. 5 bottom. Here again, the drain end of the channel is highly sensitive to P_{av}. This trend can be traced back to the nonlinearity introduced by velocity saturation, but the DC current reduction in class A cannot be ascribed only to this effect, since it is not observed in trap-free devices including velocity saturation. Hence we concentrate on the Fe-doped region below the channel, e.g. the point marked in red. As shown in Fig. 6, at high power ($P_{\text{av}} = 15$ dBm, i.e. $P_{\text{out}} = 30$ dBm) the electron density is a highly nonlinear, clipped waveform, with a significant DC component. Despite its very low value, the density varies in time, being partly *above* and partly *below* n_1, the electron density when the Fermi energy equals the trap level. According to SRH theory, when $n > n_1$ electron trapping prevails, whereas emission prevails for $n < n_1$. Thus, the time-varying electron density makes the trap concentration dynamically adapt to the average electron concentration, which in turn highly depends on P_{av}. As shown in Fig. 7, despite the electron density is very low, trap occupation varies significantly from back-off to high power, hence building up a significant charge and affecting the overall device electric field. Notice that both electrons and n_1 highly depend on T, but the trap occupation is not so sensitive: this is why the relative variation of the DC current with increasing power is independent of T (Fig. 4, right).

As reported in Fig. 3 right, the class AB stage behavior is less influenced by trap dynamics [13]. In fact, here the DC

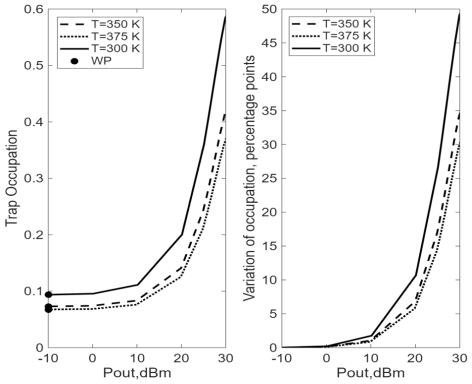

Fig. 7: Class A trap occupation vs. output power for the selected point in the drain depleted region.

current drop is compensated by the rectifying stage behavior, as in class A at high power (not shown for brevity). Overall, the proposed framework demonstrates the capability of the tool to probe trap related phenomena extremely complicated to investigate only from experiments.

References

[1] N. K. Subramani, "Physics-based TCAD device simulations and measurements of GaN HEMT technology for RF power amplifier applications," Ph.D. dissertation, University of Limoges, 2017. [Online]. Available: https://tel.archives-ouvertes.fr/tel-01702325

[2] A. Raffo *et al.*, "Characterization of GaN HEMT low-frequency dispersion through a multiharmonic measurement system," *IEEE Trans. on Microwave Theory and Techniques*, vol. 58, no. 9, pp. 2490–2496, Sep. 2010.

[3] J. C. Pedro *et al.*, "A physics-based 1-D equivalent circuit model for an AlGaN/GaN HEMT," *IEEE Trans. on Microwave Theory and Techniques*, vol. 72, no. 10, pp. 5615–5623, Oct. 2024.

[4] G. Meneghesso *et al.*, "Reliability of GaN high-electron-mobility transistors: State of the art and perspectives," *IEEE Trans. on Device and Materials Reliability*, vol. 8, no. 2, pp. 332–343, Jun. 2008.

[5] N. Zagni *et al.*, "Temperature-independent current dispersion in 0.15 μm AlGaN/GaN HEMTs for 5G applications," *Micromachines*, vol. 13, no. 12, p. 2244, Dec 2022.

[6] E. Catoggio *et al.*, "Efficient TCAD thermal analysis of semiconductor devices," *IEEE Trans. on Electron Devices*, vol. 68, no. 11, pp. 5462–5468, Nov. 2021.

[7] S. Donati Guerrieri *et al.*, "Variability-aware MMIC design through multiphysics modelling," in *2022 IEEE MTT-S International Conference on Numerical Electromagnetic and Multiphysics Modeling and Optimization (NEMO)*. IEEE, Jul. 2022, pp. 1–4.

[8] S. Donati Guerrieri *et al.*, "A unified approach to the sensitivity and variability physics-based modeling of semiconductor devices operated in dynamic conditions—Part I: Large-signal sensitivity," *IEEE Trans. on Electron Devices*, vol. 63, no. 3, pp. 1195–1201, Mar 2016.

[9] ——, "A unified approach to the sensitivity and variability physics-based modeling of semiconductor devices operated in dynamic conditions.—Part II: Small-signal and conversion matrix sensitivity," *IEEE Trans. on Electron Devices*, vol. 63, no. 3, pp. 1202–1208, Mar 2016.

[10] F. Bonani and G. Ghione, *Noise in Semiconductor Devices*. Springer Berlin Heidelberg, 2001.

[11] "Synopsys Sentaurus," https://www.synopsys.com/.

[12] P. V. Raja *et al.*, "Identification of buffer and surface traps in Fe-doped AlGaN/GaN HEMTs using Y21 frequency dispersion properties," *Electronics*, vol. 10, no. 24, p. 3096, Dec 2021.

[13] O. Jardel *et al.*, "An electrothermal model for AlGaN/GaN power HEMTs including trapping effects to improve large-signal simulation results on high VSWR," *IEEE Trans. on Microwave Theory and Techniques*, vol. 55, no. 12, pp. 2660–2669, Dec. 2007.